

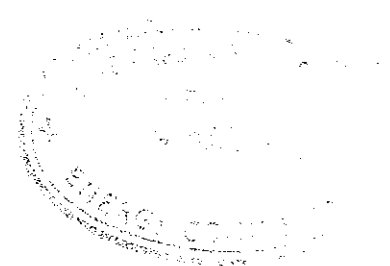


**AUSTRALIAN ATOMIC ENERGY COMMISSION
RESEARCH ESTABLISHMENT
LUCAS HEIGHTS**

**NON-STATISTICAL EFFECTS IN THE RADIATIVE CAPTURE
CROSS SECTIONS OF THE NEODYMIUM ISOTOPES****

by

**A.R. de L. MUSGROVE
B.J. ALLEN
J.W. BOLDEMAN
*R.L. MACKLIN**



****Research sponsored in part by ERDA under contract with
Union Carbide Corporation**

***Oak Ridge National Laboratory, Oak Ridge, Tenn. USA**

January 1977
ISBN 0 642 99769 1

AUSTRALIAN ATOMIC ENERGY COMMISSION
RESEARCH ESTABLISHMENT
LUCAS HEIGHTS

NON-STATISTICAL EFFECTS IN THE RADIATIVE CAPTURE
CROSS SECTIONS OF THE NEODYMIUM ISOTOPES[†]

by

A.R. de L. MUSGROVE
B.J. ALLEN
J.W. BOLDEMAN
* R.L. MACKLIN

ABSTRACT

The neutron capture cross sections of the stable neodymium isotopes have been measured with high energy resolution in the keV region at the 40 m station of ORELA. Average resonance parameters are extracted for s-wave resonances.

Significant positive correlations are found between Γ_n^0 and Γ_γ for all isotopes. The magnitude of the observed correlation coefficient, particularly for ^{142}Nd ($\rho = 0.9$), cannot be explained in terms of valence neutron capture and additional mechanisms are discussed.

The average s-wave radiative widths for the odd-A isotopes are markedly greater than for the even-A isotopes, while the p-wave radiative width for ^{142}Nd is considerably less than the s-wave width.

[†] Research sponsored in part by ERDA under contract with Union Carbide Corporation.

* Oak Ridge National Laboratory, Oak Ridge, Tenn. USA

National Library of Australia card number and ISBN 0 642 99769 1

The following descriptors have been selected from the INIS Thesaurus to describe the subject content of this report for information retrieval purposes. For further details please refer to IAEA-INIS-12 (INIS: Manual for Indexing) and IAEA-INIS-13 (INIS: Thesaurus) published in Vienna by the International Atomic Energy Agency.

CAPTURE; CROSS SECTIONS; EXCITED STATES; keV RANGE; NEODYMIUM 142;
NEODYMIUM 143; NEODYMIUM 144; NEODYMIUM 145; NEODYMIUM 146; NEODYMIUM 148;
NEUTRON REACTIONS; P WAVES; RESONANCE; S WAVES; STATISTICS;
STRENGTH FUNCTIONS

CONTENTS

	<u>Page</u>
1. INTRODUCTION	1
2. EXPERIMENTAL DETAILS	1
3. ANALYSIS	2
4. RESULTS	3
4.1 Average s-wave Level Spacings	3
4.2 Neutron Strength Functions	4
4.3 Average Radiative Widths	4
4.4 Correlations and the Valence Theory	5
5. CONCLUSIONS	7
6. REFERENCES	8
Table 1 Target and Run Parameters	
Table 2 ^{142}Nd Resonance Parameters	
Table 3 ^{143}Nd Resonance Parameters	
Table 4 ^{144}Nd Resonance Parameters	
Table 5 ^{145}Nd Resonance Parameters	
Table 6 ^{146}Nd Resonance Parameters	
Table 7 ^{148}Nd Resonance Parameters	
Table 8 Average Resonance Parameters	
Table 9 The Level Density Parameter Calculated for the Isotopes of Neodymium	
Table 10 Calculated q_{ij} (Equation (1)) and Q_i (Equation (2)) for ^{142}Nd	
Table 11 Calculated Valence Radiative Widths for Selected Resonances in the Nd Isotopes Compared with the Average	
Figure 1 Fit to experimental data for ^{142}Nd (n, γ) between 12 and 20 keV.	
Figure 2 Cross section for ^{142}Nd (n, γ) compared with statistical model calculation	
Figure 3 Cross section for ^{143}Nd (n, γ) compared with statistical model calculation	
Figure 4 Cross section for ^{144}Nd (n, γ) compared with statistical model calculation	
Figure 5 Cross section for ^{146}Nd (n, γ) compared with statistical model calculation	

CONTENTS (Continued)

- Figure 6 Cross section for ^{148}Nd (n,γ) compared with statistical model calculation
- Figure 7 Level density parameter a/A versus the Cameron shell correction energy. Also shown is the Gilbert & Cameron global fit for undeformed nuclei.

1. INTRODUCTION

The neutron capture cross sections for the isotopes $^{142,143,144,145,146,148}\text{Nd}$ have been measured in the keV region with the high resolution ($\Delta E/E \leq 0.2\%$) available at the 40 m station of the Oak Ridge Electron Linear Accelerator (ORELA). The neodymium isotopes occur near the peak of the 4s neutron strength function, and the N=82 shell closure at ^{142}Nd ensures that final 3p levels contain appreciable fractions of the single particle configuration. Therefore, valence neutron transitions [Lynn 1968] between the initial s-wave resonances and final p-wave levels can be expected to occur in radiative neutron capture. However, in the neighbouring closed-shell nucleus ^{138}Ba , valence effects could account for neither the disparity between s- and p-wave radiative widths, nor the correlation observed between neutron and radiative widths. A further non-statistical contribution to the s-wave radiative widths was indicated [Musgrove et al. 1975]. The extension of that study to the isotopes of Nd is therefore of considerable interest in the study of possible doorway state contributions to radiative capture widths.

The nucleus ^{142}Nd is of further interest from an astrophysical viewpoint since it, along with ^{134}Ba and ^{136}Ba (see discussion in Musgrove et al. 1976a), is formed exclusively by the s-process of nucleosynthesis [Burbidge et al. 1957]. The solar system abundance of ^{142}Nd is thus inversely related to the kilovolt neutron capture cross section and the present measurement is the first information relating to this cross section. Previously, semi-empirical estimates, which were subject to considerable uncertainties, were required for this cross section [Allen et al. 1971].

The high resolution transmission measurements of Tellier [1971] provided neutron widths for use in the analysis of the capture data, so our analysis has provided many radiative capture widths for all isotopes studied.

2. EXPERIMENTAL DETAILS

The capture γ -ray detector, located at the 40 m station of ORELA, utilised a pair of fluorocarbon liquid scintillators with low sensitivity to scattered neutrons and typically ~15 per cent efficiency for detecting the γ -ray cascade. The efficiency is made approximately independent of the γ -ray multiplicity by assigning calculated weights to the detected events as described in Macklin et al. [1971] and Macklin & Allen [1971]. The efficiency of the device was calibrated using the saturated resonance technique for the 4.9 eV resonance in ^{197}Au .

The data were corrected for dead time effects and normalised with respect to the ${}^6\text{Li}(n,\alpha)$ cross section as described in previous papers (listed in some detail in Boldeman *et al.* [1975]). The absolute error in normalisation for the present runs is expected to be better than 10 per cent and we have assumed a 10 per cent normalisation error in the quoted results. All targets in the present series were enriched oxide samples, details of which appear in Table 1.

3. ANALYSIS

A typical sample of the experimental data is given for ${}^{142}\text{Nd}$ in Figure 1 along with the calculated fit. The analysis (described in more detail in Musgrove *et al.* [1974]) uses a Monte Carlo code [Sullivan *et al.* 1969] to correct each resonance in the capture yield data for multiple-scattering and self-shielding effects. An iterative fit to the observed capture area is performed by varying the smaller of the input guesses for Γ_γ and Γ_n and finally the corrected capture kernel $g\Gamma_n\Gamma_\gamma/\Gamma$ is obtained. The time-dependent background is assumed to be linear beneath each resonance and a further correction is sometimes required to account for prompt detection of neutrons. In the present case, this correction can be ignored in comparison with other sources of uncertainty. The multiple-scattering correction is also negligible and the Γ_n values supplied by Tellier [1971] allow a close estimate for the self-shielding losses. Statistical errors are typically <3 per cent and so contribute little to the overall error. The quoted errors for resonance energies are determined from the consistency between our data and those of Tellier and are not meant to represent the accuracy with which we can determine the centre of the resonance peak, which is considerably less than the quoted errors.

In most cases, the neutron widths of Tellier gave fits consistent with our data and therefore we did not attempt to extract a neutron width from a resonance-shape analysis in those cases. However, some exceptions are noted. The Γ_n data of Tellier are generally more accurate than we could provide.

For resonances having $\Gamma_n < \Gamma_\gamma$, the average value of Γ_γ was used in our analysis to determine $g\Gamma_n$. The agreement between our data and those of Tellier is not so good for these resonances which can be difficult to analyse accurately in transmission.

We detected a number of resonances not seen by Tellier, and most of these we ascribe to p-wave neutron capture, for which the sensitivity of the present experiment is far greater than in transmission. Also, particularly in ${}^{142}\text{Nd}$, we assigned some resonances as p-wave which *were* observed

in transmission. We assumed that all resonances having $g\Gamma_n\Gamma_\gamma/\Gamma \geq 1.7 \langle\Gamma_\gamma\rangle$ had spin weighting factor $g = 2$ for our analysis. This assignment was in most cases strengthened by a small neutron width measured in transmission which gave high p-wave probability from a Bayes' theorem test, as described in Musgrove et al. [1974].

We were also guided in some spin assignments by probabilities based on the Wigner level spacing distribution. In cases where two levels are spaced more closely than $\langle D \rangle / 10$, there is less than 1 per cent chance that they belong to the same (ℓ, J) sequence. Hence, if one is known to be s-wave, the other is likely to be p-wave.

For the odd-A isotopes, Tellier gave only values for $g\Gamma_n$ and our analysis proceeded by assuming $g = 0.5$ and the appropriate Γ_n .

Capture cross sections averaged over convenient energy ranges were obtained by summing the calculated capture areas $A_\gamma = 2\pi^2 \kappa^2 \Gamma_n\Gamma_\gamma/\Gamma$, in regions where few resonances were undetected. Above that energy, the background was subtracted and average self-shielding and multiple-scattering corrections were applied to the integrated capture yield to obtain the capture cross section. At high energies, the uncertainty in the background subtraction is an increasing factor in the cross section error. The measured cross sections are given in Figures 2-6 and are compared with a calculated statistical model cross section using the best set of average resonance parameters for each isotope. For ^{145}Nd , the high level density made the background subtraction technique uncertain, and even summing the capture areas of the observed resonances leads to a considerable under-estimation of the cross section, owing to missed levels.

4. RESULTS

The resonance parameters for the observed resonances are given in Tables 2-7 and compared with the data of Tellier [1971]. The average resonance parameters from the current data are given in Table 8 and are discussed briefly below. Also given are the average 30 keV capture cross sections since they are of astrophysical interest.

4.1 Average s-wave Level Spacings

The average s-wave level spacing is an important parameter in cross sectional calculations. The systematics have been studied using a modified free-gas approach by Gilbert & Cameron [1965] who found that the level density parameter a , related to the density of single particle states near the Fermi energy, was proportional to the shell correction energy found in semi-empirical mass laws. In Table 9 calculated values for the level density

parameter for the Nd isotopes are compared with the values obtained in the same exercise by Karzhavina *et al.* [1969].

Also, for comparison, this parameter was calculated for neighbouring isotopes of Ba [Musgrove *et al.* 1976b] and Eu [Rahn *et al.* 1972]. The quantity a/A is plotted versus the Cameron shell correction energy [Cameron 1958] in Figure 7, along with the Gilbert & Cameron universal fit for undeformed nuclei [Gilbert & Cameron 1965]. All but one of the Nd isotopes fall below the line, as do all the Sm isotopes. On the other hand, the Ba and Eu isotopes lie above the line. A simple correction procedure involving an alteration to either the pairing or shell energy for each Z value could improve the fit to the data. There are also some indications that even-odd effects have not been fully removed.

4.2 Neutron Strength Functions

The s-wave neutron strength functions given in Table 8 are mostly based on neutron widths from Tellier [1971], however our values for ^{145}Nd and ^{146}Nd are somewhat greater than his. We also obtained p-wave neutron strength functions for $^{142,143}\text{Nd}$ and ^{144}Nd which are in line with the trend established in the Ba isotopes [Musgrove *et al.* 1976b]. A penetrability radius $R = 1.35 A^{1/3} \text{ f}$ was used to calculate the reduced p-wave neutron widths and, in each case, a correction of order 10-15 per cent was made for missing weak levels.

4.3 Average Radiative Widths

In ^{142}Nd , we find a considerable enhancement of s-wave radiative widths over the p-wave widths. Comparison with ^{138}Ba , a neighbouring closed shell nucleus, shows that the amount of enhancement has decreased sharply, as has the average s-wave level spacing. Average p-wave radiative widths could not be obtained for the other Nd isotopes.

The ^{144}Nd s-wave width is close to the p-wave width found for ^{142}Nd , whereas both odd- A nuclei have significantly greater radiative widths than their even- A neighbours. No such even-odd effect is predicted by the semi-empirical formulae designed to give statistical model radiative widths [Benzi *et al.* 1974].

Previous measurements of radiative width at lower neutron bombarding energies do not show a significant even-odd effect [Karzhavina *et al.* 1969, Rohr *et al.* 1971, Mughabghab & Garber 1973]. Our width for ^{143}Nd is about 10 meV greater than the low-energy average but, for ^{145}Nd , our value is about 20 meV greater than the previous average. In addition, our radiative widths for $^{144,146,148}\text{Nd}$ tend to be somewhat smaller (by 10 meV)

than the average of the earlier measurements [Karzhavina et al. 1969].

4.4 Correlations and the Valence Theory

The high correlation coefficient $\rho(\Gamma_n^0, \Gamma_\gamma) = 0.9$ found in ^{142}Nd for 24 resonances is strongly influenced by the large values for both widths from the 30610 eV resonance. It is of considerable interest to calculate the total valence width for this resonance using the optical model [Lane & Mughabghab 1974] and the formalism of another paper [Musgrove et al. 1976c]. The valence width between initial and final single particle states, labelled i and j , can be written :

$$\Gamma_{\gamma ij}^V = q_{ij} E_{\gamma ij}^2 \cdot Z^2/A^2 \cdot \theta_j^2 \Gamma_{ni}^0 \quad , \quad \dots (1)$$

where E_γ is the γ -ray energy, θ_j^2 is the final state spectroscopic factor and Γ_{ni}^0 is the reduced neutron width for the s -wave initial state. The quantity q_{ij} is calculated from the optical model and contains radial and angular integration parts of the dipole matrix element. Summing Equation (1) over final $p_{1/2}$, $p_{3/2}$ levels, using spectroscopic factors from Christensen et al. [1967], Nealy & Sheline [1967] and Booth & Wilson [1975], we write :

$$\Gamma_{\gamma i}^V = Q_i \Gamma_{ni}^0 \quad . \quad \dots (2)$$

The calculated values for q_{ij} , Q_i are given in Table 10 for ^{142}Nd . The q_{ij} are energy dependent, decreasing with increasing bombarding energy as shown in Allen et al. [1976]. The value quoted was calculated for $E_n = 10$ keV.

The reduced neutron width for the 30610 eV resonance is 2.09 eV and, using the Q_i in Table 10, the total valence width for this resonance is found to be 73 meV. Although large compared with the average s -wave radiative width in ^{142}Nd , it accounts for less than 20% of the γ -decay for this resonance.

For the other neodymium isotopes, a rough estimate can be made for the valence component of radiative widths using the value $Q_i \approx 0.035$, found for ^{142}Nd . In Table 11 the calculated valence widths are given for the largest resonances in each isotope and, for comparison, the calculated average valence width as given by :

$$\langle \Gamma_{\gamma i}^V \rangle = Q_i S_o \langle D \rangle \quad , \quad \dots (3)$$

where S_0 is the s-wave neutron strength function and $\langle D \rangle$ the average level spacing.

The observed correlation coefficients $\rho(\Gamma_n^0, \Gamma_\gamma)$ are considerably greater than expected on the basis of the valence theory. In particular, ^{142}Nd has the greatest measured correlation coefficient ($\rho = 0.9$), yet a Monte Carlo simulation, which *included* a valence term in the radiative width, found less than 0.5% chance of measuring a correlation coefficient $\rho(\Gamma_n^0, \Gamma_\gamma)$ greater than 0.8.

Evidently a further contribution to the s-wave radiative widths is responsible for the large radiative width enhancement found in ^{142}Nd and, in particular, for the 30610 eV resonance in ^{142}Nd . The process has a transition probability proportional to the reduced neutron width in the initial state and could be interpreted qualitatively as one where the incident neutron in the entrance channel undergoes an E1 transition, to a particle-hole excited state in the final nucleus, as described by Beer [1971].

If the final state correlations were found to be low, the existence of initial state correlations could be attributed to the presence, in the final p-wave states, of (p-h) configurations coupled with the 4s incident neutron, which would be fed directly from the entrance channel.

Alternatively, one could envisage the entrance channel wave function having several target excitation components. The proton configuration of neodymium is not magic, so there are a number of possible orbits for the protons to occupy near $Z \approx 60$. Since, in general, different proportions of these configurations are present in the final states (after γ de-excitation) it is possible to reproduce any measured correlation coefficient by suitably adjusting phases and magnitudes of the various configurations in initial and final states.

To give two examples of the latter process; the ^{28}Si data near 750 keV have recently been interpreted [Halderson et al. 1976] in terms of valence capture wherein the measured neutron widths have been reduced by an out-of-phase component which does not contribute to the γ -ray widths (*i.e.* the valence calculation will underestimate the magnitude of the valence width). On the other hand, the ^{98}Mo data was interpreted [Musgrove et al. 1976c] as showing that the measured neutron widths had been increased by a significant in-phase component which resulted in the valence effect being overestimated.

A decision between the alternative mechanisms proposed above, would require γ -ray spectra measurements (particularly for the ^{142}Nd 30610 eV

resonance). The thermal capture cross sections of ^{142}Nd and ^{144}Nd (18.7 b and 5 b respectively) indicate, in each case, that the thermal capture data reflect the decay properties of nearby s-wave resonances. The thermal capture spectrum for ^{142}Nd [Gelletly 1974, Mirza et al. 1975] is somewhat different to that observed from the neighbouring ^{138}Ba and ^{140}Ce [Gelletly 1974] which have low thermal cross sections, but the strong E1 lines to final p-wave states typical of direct capture. In ^{142}Nd more strength is taken up by transitions to the more highly excited levels containing the single particle final state configuration. Depending on the choice of final state spectroscopic factors [Christensen et al. 1967, Nealy & Sheline 1967, Booth & Wilson 1975] the correlation coefficient between reduced γ -ray intensities and final state spectroscopic factors can range between 0 and 0.6.

The final state correlation coefficient for the thermal transition strengths [Najam et al. 1975] of ^{144}Nd is only 0.2 ± 0.3 . In neither case can one decide definitely, on the basis of the final state correlation coefficient, which of the alternative mechanisms is responsible for the initial state correlations observed in these nuclei.

We remark finally the apparent presence of correlations in the odd-A isotopes, $^{143}, ^{145}\text{Nd}$. These are enclosed in parentheses in Table 8 since the quantity calculated was $\rho(g\Gamma_n^0, g\Gamma_\gamma)$. For ^{143}Nd , several low energy resonances have measured J, Γ_n and Γ_γ [Rohr et al. 1975]. The fourteen resonances with $J^\pi = 4^-$ have a measured correlation coefficient $\rho(\Gamma_n^0, \Gamma_\gamma) = 0.34$, while the seven resonances with $J^\pi = 3^-$ show zero correlation. Significantly, the neutron strength function for the $J^\pi = 4^-$ resonances is almost twice that for the $J^\pi = 3^-$ levels.

5. CONCLUSIONS

The present study of radiative capture in the neodymium isotopes has increased the range of mass numbers over which correlations of the type $\rho(\Gamma_n^0, \Gamma_\gamma)$ have been observed. The usual valence model appears to be unable to explain the magnitude of the correlations and a further process must be involved.

The s-wave radiative widths also show a significant even-odd effect which cannot be explained in current statistical models.

6. REFERENCES

- Allen, B.J., Gibbons, J.H. & Macklin, R.L. [1971] - *Advances in Nuclear Physics*, Vol. 4. Plenum Press, p.205.
- Allen, B.J., Musgrove, A.R. de L., Boldeman, J.W., Kenny, M.J. & Macklin, R.L. [1976] - *Nucl. Phys.*, A269:408.
- Barrett, R.F. & Terasawa, T. [1974] - *Nucl. Phys.*, A240:442.
- Beer, M. [1971] - *Ann. Phys.*, 65:181.
- Benzi, V., Reffo, G. & Vaccari, M. [1974] - Proc. Panel on Fission Product Nuclear Data, IAEA Vol. III, p.123.
- Boldeman, J.W., Allen, B.J., Musgrove, A.R. de L. & Macklin, R.L. [1975] - *Nucl. Phys.*, A246:1.
- Booth, W. & Wilson, S. [1975] - *Nucl. Phys.*, A238:301.
- Burbidge, E.M., Burbidge, G.R., Fowler, W.A. & Hoyle, F. [1957] - *Rev. Mod. Phys.*, 29:547.
- Cameron, A.G.W. [1958] - *Can. J. Phys.*, 36:1040.
- Christensen, P.R., Herskind, B., Borchers, R.R. & Westgaard, L. [1967] - *Nucl. Phys.*, A102:481.
- Gelletly, W. [1974] - *J. Phys.*, A7 :128.
- Gilbert, A. & Cameron, A.G.W. [1965] - *Can. J. Phys.*, 43:1446.
- Halderson, D., Castel, B., Johnstone, I.P. & Divadeenam, M. [1976] - *Phys. Rev. Lett.*, 36:760.
- Karzhavina, E.N., Fong, N.N., Popov, A.B. & Taskaev, A.I. [1969] - *Sov. Nucl. Phys.*, 8:371.
- Lane, A.M. & Mughabghab, S.F. [1974] - *Phys. Rev.*, C10:412.
- Lynn, J.E. [1968] - *Theory of Neutron Resonance Reactions*, Clarendon Press, Oxford.
- Macklin, R.L. & Allen, B.J. [1971] - *Nucl. Instrum. Methods*, 91:565.
- Macklin, R.L., Hill, N.W. & Allen, B.J. [1971] - *Nucl. Instrum. Methods*, 96:506.
- Mirza, J.A., Khan, A.M., Irshad, M., Schmidt, H.A., Ishaq, A.F.M. & Anwar-ul-Islam, M. [1975] - Proc. 2nd Int. Symp. on Neutron Capture Gamma Ray Spectroscopy, Petten. IAEA, p.557.
- Mughabghab, S.F. & Garber, D.I. [1973] - BNL-325, 3rd Ed., Vol. 1.
- Musgrove, A.R. de L., Allen, B.J. & Macklin, R.L. [1974] - AAEC/E327.
- Musgrove, A.R. de L., Allen, B.J., Boldeman, J.W. & Macklin, R.L. [1975] - *Nucl. Phys.*, A252:301.
- Musgrove, A.R. de L., Allen, B.J., Boldeman, J.W. & Macklin, R.L. [1976a] - *Nucl. Phys.*, A256:173.

- Musgrove, A.R. de L., Allen, B.J., Boldeman, J.W. & Macklin, R.L. [1976b] - *Aust. J. Phys.*, 29:157.
- Musgrove, A.R. de L., Allen, B.J., Boldeman, J.W. & Macklin, R.L. [1976c] - *Nucl. Phys.*, A270:108.
- Najam, M.R., Ishaq, A.F.M., Anwar-ul-Islam, M., Khan, A.M. & Mirza, J.A. [1975] - Proc. 2nd Int. Symp. on Neutron Capture Gamma Ray Spectroscopy, Petten, IAEA, p.566.
- Nealy, C.L. & Sheline, R.K. [1967] - *Phys. Rev.*, 155:1314.
- Rahn, F., Camarda, H.S., Hacken, G., Havens, W.W., Liou, H.I., Rainwater, J., Slagowitz, M. & Wynchank, S. [1972] - *Phys. Rev.*, C6:251.
- Rohr, G., Weigmann, H. & Weske, M. [1971] - Proc. Conf. on Neutron Cross Sections and Technology, Knoxville, 2:743.
- Rohr, G., van der Veen, T., Weigmann, H. & Winter, J. [1975] - Proc. 2nd Int. Symp on Neutron Capture Gamma Ray Spectroscopy, Petten. IAEA, p.306.
- Sullivan, J.G., Warner, G.G., Block, R.C. & Hockenbury, R.W. [1969] - Rensselaer Polytechnic Institute unpublished report RPI-328-155.
- Tellier, H. [1971] - CEA-N-1459.

TABLE 1

TARGET AND RUN PARAMETERS

	^{142}Nd	^{143}Nd	^{144}Nd	^{145}Nd	^{146}Nd	^{148}Nd
Isotopic enrichment (%)	88	91	98	92	90	96
Isotopic thickness (atoms b^{-1})	0.0069	0.0080	0.0086	0.0081	0.0073	0.0076
Pulse width (ns)	8	5	8	5	8	8

TABLE 2
 ^{142}Nd RESONANCE PARAMETERS

E (eV)	$g\Gamma_n\Gamma_\gamma/\Gamma$ (meV)	$g\Gamma_n$ (meV)	Γ_n (meV) f)	Γ_γ (meV)	ℓ	g
2632±1	10±1.5	12±1	20.0±7.5		1 ^{e)}	
2767	^{144}Nd or ^{143}Nd impurity		62.5±20			
3267±3	15±2	22±5	-		(1) ^{e)}	
3377±3	38±4	(300) ^{d)}	-	43±10	(0) ^{e)}	
3989±3	47±5	(780) ^{d)}	780±400 ^{a)}	50±6	(0) ^{f)}	
4141±3	22±3	39±10	5.5±2.0		1 ^{e)}	
4502±2	1.8±0.3	1.8±0.3	-		1 ^{e)}	
4522±2	44±5	7500±1000	7700±350	44±5	0 ^{f)}	
4948±3	- ^{b)}	-	105±20			
5052±3	40±4		-			
5144±3	47±5		-			
5412±3	50±6	(110)	110±15	45±10	1	(2) ^{c)}
5475±2	41±5	(3500)	3500±200	41±5	0 ^{f)}	
5669	- ^{b)}	-	110±15			
5943±3	3.7±0.8	4±1	-		1 ^{e)}	
5967±3	44±5	(1393) ^{d)}	1393±75	45±5	0 ^{f)}	
6220±4	58±6		-		1	(2) ^{c)}
6908±4	47±5	(525) ^{d)}	525±150	53±8	(0)	
6936±4	18±3	29±8	-		1 ^{e)}	
7228±4	45±5	(500) ^{d)}	500±150	50±8	(0)	
8236±4	32±4	(500) ^{d)}	500±150	34±8		
8395±4	45±5	(1900) ^{d)}	1900±200	47±6	0 ^{f)}	
8780±4	64±7	(500) ^{d)}	500±150	37±6	1	(2) ^{c)}
8990±4	47±5		-		(0)	
9807±4	70±8	(500) ^{d)}	-	40±10	1	(2) ^{c)}
9850±4	64±7	1200±3000	11780±1250	64±7	0 ^{f)}	

TABLE 2 (Cont'd)

E (eV)	$g\Gamma_n \Gamma_\gamma / \Gamma$ (meV)	$g\Gamma_n$ (meV)	Γ_n (meV) f)	Γ_γ (meV)	l	g
10118±5	78±8	(1000) ^{d)}	-	43±10	1	(2) ^{c)}
10260±5	16±2	20±5	-		1 ^{e)}	
10925±5	43±5	(10500) ^{d)}	10500±1000	43±5	0 ^{f)}	
11100±5	46±5		-		1	(2)
11220±5	27±4		-			
11443±5	36±4		-			
12885±6	84±9		-		1	(2) ^{c)}
13395±6	49±6		-			
13490±7	84±9	(4200) ^{d)}	4200±1000	86±10	0 ^{f)}	
13600±10	234±30	90000±10000	89225±9000	235±30	0 ^{f)}	
14205±8	35±4		-			
14430±8	55±7		-			
14930±8	10±5	13±6	-		1 ^{e)}	
15005±10	68±8		-		1	(2) ^{e)}
15390±10	43±8	(12850) ^{d)}	12850±1500	43±8	0 ^{f)}	
15590±10	53±6		-			
15865±20	87±9	(400) ^{d)}	-	55±10	1	(2) ^{c)}
16190±10	91±20	(54100) ^{d)}	54100±5000	91±20	0 ^{f)}	
16290±10	82±8	(600) ^{d)}	-	48±10	1	(2) ^{c)}
17000±10	89±9	(2630) ^{d)}	2630±500	46±5	(1)	(2) ^{c)}
17280±10	56±7		-			
18000±10	40±7		-			
19000±10	77±8		-			
19180±10	26±6		-			
19260±10	78±15	(45600) ^{d)}	46500±5000	78±15	0 ^{f)}	
19530±10	20±7		-			
19860±10	53±9		-			

TABLE 2 (Cont'd)

E (eV)	$g_n^{\Gamma} \Gamma_{\gamma} / \Gamma$ (meV)	g_n^{Γ} (meV)	Γ_n (meV f)	Γ_{γ} (meV)	ℓ	g
20125±10	100±15				(1)	(2) ^{c)}
20375±10	50±10					
20555±10	70±10					
20725±10	21±8					
20795±10	23±6					
21150±10	98±15	(24380)	24380±2500	98±15	0 ^{f)}	
21420±10	41±7					
21615±10	26±7					
21690±10	102±12				(1)	(2) ^{c)}
21955±10	47±8	(12000)	11978±1250	48±8	0 ^{f)}	
22370±10	109±13				(1)	(2) ^{c)}
22515±10	42±7					
22740±10	70±9					
23285±10	79±10					
23740±10	82±11					
23995±10	120±18				(1)	(2) ^{c)}
24170±10	30±8					
24300±10	23±7					
24380±10	57±9					
24422±10	42±7					
24480±10	20±6					
24655±10	20±8					
24730±10	54±9					
24985±10	66±10	(4200)	4200±1000	67±10	0 ^{f)}	
25280±10	54±10					

TABLE 2 (Cont'd)

E (eV)	$g\Gamma_n \Gamma_\gamma / \Gamma$ (meV)	$g\Gamma_n$ (meV)	Γ_n (meV f)	Γ_γ (meV)	ℓ	g
25400±10	88±11					
25620±10	55±8					
25700±10	81±10					
25760±10	48±7	(25700)	25670±3000	48±7	0 ^{f)}	
26450±10	101±15				(1)	(2) ^{c)}
26580±10	183±22	(21050)	21050±2500	185±25	0 ^{f)}	
27310±10	106±18				(1)	(2) ^{c)}
27730±10	59±18					
28220±10	134±17					
29710±10	114±14					
30210±10	86±12					
30610±30	435±50	(364650)	364650±50000	435±50	0 ^{f)}	
30740±10	86±10	(29000)	29000±5000	86±10	0 ^{f)}	
31270±10	82±10					
31458±10	149±25					
31655±10	137±25					
31940±10	106±20					

a) Value given in Karzhavina *et al.* [1969] but not included in compilation of Mughabghab & Garber [1973].

b) Not present in our data.

c) Assumed g=2 from value of $g\Gamma_n \Gamma_\gamma / \Gamma$ and Γ_n upper limit from Tellier [1971].

d) Approximate or assumed value.

e) From Bayes' theorem calculation (confidence level > 98%).

f) From Tellier [1971].

TABLE 3
¹⁴³Nd RESONANCE PARAMETERS

E (eV)	$g\Gamma_n \Gamma_\gamma / \Gamma$ (meV)	$2g\Gamma_n$ (meV)	$2g\Gamma_n$ (meV b)	$2g\Gamma_\gamma$ (meV)	g a)
2594±3	6.6±0.7	17±3			1
2611±3	4.2±0.4	9±2			1
2634±3	62±6	(2840)	2840±100	130±15	0
2706±3	6.1±0.6	14±3			1
2715±3	31±3	(720)	720±40	68±9	0
2761±3	49±5	(6340)	6340±300	100±15	0
2798±3	6.2±0.7	14±3			1
2811±3	18±2	(325)	325±30	40±6	0
2822±3	23±3	100±30			(0)
2868±3	26±3	135±40			(0)
2877±3	52±6	(3270)	3270±120	108±13	0
2914±3	28±3	(1085)	1085±60	58±7	0
2967±3	4.5±0.6	9±2			1
2998±3	20±2	76±10			(0)
3040±3	12±1	33±6			1
3046±3	53±5	(2830)	2830±100	111±16	0
3074±3	45±5	(1035)	1035±60	99±15	0
3119±3	33±4	(555)	555±50	76±11	0
3186±3	47±5	(2380)	2380±100	98±15	0
3198±3	39±4	(560)	560±50	92±14	0
3234±3	36±4	(1570)	1570±80	75±10	0
3280±3	18±2	62±20			1
3295±3	60±6	2400±800	1625±90	125±15	0
3322±3	3±1	6.5±2			1
3366±3	5.5±1	14±2			1
3386±3	39±4	(2300)	2300±100	81±11	0

TABLE 3 (Cont'd)

E (eV)	$g\Gamma_n \Gamma_\gamma / \Gamma$ (meV)	$2g\Gamma_n$ (meV)	$2g\Gamma_n$ (meV b)	$2g\Gamma_\gamma$ (meV)	λ
3429±3	33±4	(215)	215±30	95±13	0
3458±3	27±3	150±50			
3465±3	33±3	(975)	975±60	71±10	0
3498±3	20±3	~70			(1)
3512±2	37±4	(1690)	1690±100	76±10	0
3545±3	7±1	17±3			1
3569±3	28±3	(250)	250±50	71±10	0
3632±3	36±4	(1670)	1670±100	75±10	0
3648±3	25±3	120±50			(0)
3696±3	10±2	26±4			1
3707±3	48±5	(2370)	2370±120	101±15	0
3719±3	37±4	(2060)	2060±120	76±10	0
3738±3	5±1	11±3			1
3746±3	5±1	12±3			1
3771±3	14±2	42±8			(1)
3782±3	28±3	(440)	440±60	64±10	0
3840±3	30±3	(225)	225±45	84±10	0
3886±3	38±4	(1120)	1120±80	81±10	0
3900±3	23±3	100±30			
3917±3	8±1	20±3			1
3958±3	39±4	(550)	550±60	92±12	0
4011±3	8±1	20±3			1
4022±3	58±6	(4380)	4380±200	120±15	0
4033±3	35±4	(1770)	1770±120	72±10	0
4050±3	9±1	23±4			1
4064±3	41±5	(2340)	2340±120	84±11	0
4089±3	11±2	30±6			1
4111±3	34±4	(215)	215±60	99±16	0

TABLE 3 (Cont'd)

E (eV)	$g\Gamma_n \Gamma_\gamma / \Gamma$ (meV)	$2g\Gamma_n$ (meV)	$2g\Gamma_n$ (meV b)	$2g\Gamma_\gamma$ (meV)	ℓ
4136±3	34±4	(970)	970±100	73±10	0
4145±3	32±4	(910)	910±100	69±10	0
4200±3	6±1	14±2			1
4209±3	13±2	37±8			1
4213±3	47±5	(6480)	6480±300	95±12	0
4247±3	32±4	(1240)	1240±100	68±10	0
4337±3	36±4	(3240)	3240±150	74±10	0
4342±3	30±4	200±50			
4399±3	28±3	(230)	230±50	74±12	0
4420±3	47±5	(1500)	540±75	101±15	0
4430±3	4±1	9±2			1
4445±3	7±1	17±3			1
4463±3	26±3	135±40			
4478±3	35±4	(730)	730±90		0
4521±3	29±3	(240)	240±60	76±10	0
4560±3	25±3	(250)	250±50	64±10	0
4601±3	36±4	(750)	750±100	79±10	0
4612±3	53±6	(1160)	1160±100	116±20	0
4663±3	18±2	62±10			
4691±3	34±4	(2630)	2630±150	69±10	0
4731±3	22±3	90±30			
4749±3	50±5	~ 2000	720±70	105±13	0
4782±3	9±1	23±4			1
4836±3	35±4	~400			
4846±3	53±6	(5450)	5450±300	108±13	0
4897±3	41±5	(6200)	6200±300	84±10	0
4909±3	10±2	26±5			1

TABLE 3 (cont'd)

E (eV)	$g_n \Gamma_\gamma / \Gamma$ (meV)	$2g_n \Gamma$ (meV)	$2g_n \Gamma$ (meV) b)	$2g_\gamma \Gamma$ (meV)	λ
4934±3	26±3	135±40			
4966±3	6±1	14±2			1
4992±3	43±5	(5070)	5070±300	89±12	0
5004±3	12±2	33±7			1
5017±3	39±4	(1780)	1780±180	82±12	0

a) λ -values determined by Bayes' theorem calculation (> 98% confidence level).

b) From Tellier [1971].

TABLE 4
¹⁴⁴Nd RESONANCE PARAMETERS

E (eV)	$g\Gamma_n\Gamma_\gamma/\Gamma$ (meV)	$g\Gamma_n$ (meV)	Γ_n (meV) d)	Γ_γ (meV)	$\ell^{a)}$	g
2762±2	63±10	4000±1000	4030±200	65±10	0	
2955±2	13.5±1.5	20±5 ^{b)}			(1)	
3063±3	3±0.5	3±0.5 ^{b)}			1	
3293±3	4.2±0.5	5±0.5 ^{b)}			1	
3538±5	43±8	15500±1500	15000±750	43±8	0	
3629±3	1.0±0.8	1±1 ^{b)}			1	
3737±3	26±3	(1360)	1360±60	26±4	0	
3750±3	11±2	15±4 ^{b)}			1	
4237±3	10±2	13±3 ^{b)}				
4602±3	29±3	~80 ^{b)}				
4743±3	28±3	(275)	275±50	31±6	(0)	
4930±6	67±10	(24200)	24200±1000	67±10	0	
4955±3	34±4	~100 ^{b)}			1	
5148±3	19±3	33±7 ^{b)}			1	
5305±3	7±1	10±2 ^{b)}			1	
5650±4	39±5	(3360)	3360±200	40±5	0	
5843±4	22±3	43±8 ^{b)}			1	
6106±6	62±7	(13000)	13000±1000	62±7	0	
6138±4	25±3	56±10 ^{b)}			1	
6747±4	19±3	33±7 ^{b)}			1	
6778±4	55±6	~150 ^{b)}			1	(2) ^{c)}
6788±10	45±5	(48000)	48000±250	45±5	0	
7023±4	36±4	20±5 ^{b)}				
7055±5	35±4	(3443)	3443±350	35±4	0	
7181±4	15±2	25±5 ^{b)}			1	
7408±4	30±4	~90			1	

TABLE 4 (Cont'd)

E (eV)	$g\Gamma_n\Gamma_\gamma/\Gamma$ (meV)	$g\Gamma_n$ (meV)	Γ_n (meV) d)	Γ_γ (meV)	$l^a)$	g
7481±4	36±4	(5160)	5160±500	36±4	0	
7818±4	24±3	51±10 ^{b)}			1	
7965±4	12±2	16±4 ^{b)}			1	
8190±8	55±7	(14315)	14315±750	55±7	0	
8230±4	21±3	39±8 ^{b)}			1	
8405±4	25±3	56±10 ^{b)}			1	
8865±5	39±5	(3100)	3100±500	39±5	0	
8876±4	22±3	50±10 ^{b)}			1	
9130±4	28±4	-80 ^{b)}				
9245±4	23±4	47±9 ^{b)}				
9300±4	9±3	11±4 ^{b)}			1	
9345±4	26±4	62±12 ^{b)}				
9375±8	36±5	(36300)	36300±1750	36±5	0	
9533±3	14±3	25±5 ^{b)}			1	
9560±5	32±4	25±6 ^{b)}				
9740±10	77±9	(47850)	47850±2500	77±9	0	
9961±5	19±4	-80 ^{b)}			1	
10040±5	21±4	39±8 ^{b)}			1	
10128±5	61±7	-200 ^{b)}			1	(2) ^{c)}
10705±5	73±8	(1000)		40±10	1	(2) ^{c)}
10711±10	46±6	(58500)	58500±2500	46±6	0	
11260±5	64±7	(18530)	18530±750	64±7	0	
11410±5	60±7	(2000)		31±10	(1)	(2) ^{c)}
11660±5	31±6	(15900)	15900±1000	31±6	0	
11740±5	33±5	(1000)		35±10		

TABLE 4 (cont'd)

- a) ℓ -values determined by Bayes' theorem (> 98% confidence level).
- b) $g\Gamma_n$ calculated assuming $\langle \Gamma_\gamma \rangle = 45$ meV.
- c) $g=2$ assumed from $g\Gamma_\gamma$ for this analysis. These resonances are not seen in total cross section.

($g\Gamma_n$) - indicates assumed value

- d) From Tellier [1971].

TABLE 5
¹⁴⁵Nd RESONANCE PARAMETERS

E (eV)	$g\Gamma_n\Gamma_\gamma/\Gamma$ (meV)	Γ_n (meV)	$2g\Gamma_n$ (meV b)	$2g\Gamma_\gamma$ (meV)
2592±3	18±2			
2604±3	34±4	(560)	560±60	77±8
2623±3	19±2			
2684±3	24±3	(410)	410±45	54±7
2708±3	15±2			
2736±3	32±4	(420)	420±50	75±9
2745±3	33±4	(620)	620±60	74±8
2755±3	27±3	(600)	600±60	60±7
2781±3	55±5	(5660)	5600±400	111±12
2792±3	38±4	(3190)	3190±300	79±10
2819±3	16±2			
2839±3	79±8	3000±1000 ^{a)}	4625±250	167±25
2882±3	42±4	(2700)	2700±150	86±9
2893±3	35±4	(1095)	1095±100	74±8
2907±3	16±2			
2921±3	34±4	(940)	940±100	74±8
2935±3	85±9	(7640)	7640±300	173±20
2959±3	22±2			
2995±3	42±4	(1360)	1360±100	89±9
3005±3	17±2			
3023±3	42±4	(3100)	3100±150	85±9
3048±3	53±5	(1230)	1230±100	116±15
3064±3	40±4	(415)	415±60	99±10
3075±3	29±3	(950)	950±30	62±7
3109±3	31±3	(480)	480±50	72±8
3119±3	42±5	(1620)	1620±80	88±10

TABLE 5 (Cont'd)

E (eV)	$g\Gamma_n \Gamma_\gamma / \Gamma$ (meV)	Γ_n (meV)	$2g\Gamma_n$ (meV) b)	$2g\Gamma_\gamma$ (meV)
3146±3	11±2			
3167±3	36±4	(1500)	1500±75	77±9
3182±3	36±4			
3196±3	19±2			
3221±3	69±8	(910)	910±60	164±20
3243±3	-	-	880±100	
3252±3	56±6	(1980)	1980±120	119±15
3258±3	18±2			
3288±3	42±5	(2200)	2200±100	87±10
3307±3	36±4	(950)	950±80	78±10
3328±3	39±4	(1100)	1100±30	84±10
3346±3	19±2		30±15	
3369±3	28±3	(460)	460±45	
3395±3	31±3	(1000) ^{a)}		66±10
3406±3	31±3	(2600) ^{a)}	3600±100	64±7
3437±3	10±2			
3454±3	34±4	(810)	810±60	74±10
3477±3	34±4	(1480)	1480±80	72±9
3513±3	57±6	(1680)	1680±100	122±15
3527±3	64±7	(1500)	1500±120	141±20
3540±3	44±5	(500)		107±20
3553±3	10±2			
3592±3	26±3	(560)	560±60	57±8
3609±3	30±3	(580)	580±60	66±8
3643±3	24±3			
3663±3	35±4	(1510)	1510±150	72±9

TABLE 5 (cont'd)

E (eV)	$g\Gamma_n \Gamma_\gamma / \Gamma$ (meV)	Γ_n (meV)	$2g\Gamma_n$ (meV) b)	$2g\Gamma_\gamma$ (meV)
3683±3	36±4	(1500)	1500±100	75±9
3697±3	37±4	(550)	550±60	86±10
3747±3	71±8	(3270)	3270±120	149±18
3796±3	27±3	(1450)	1450±100	56±7
3817±3	36±4	(1770)	1770±120	76±9
3824±3	34±4			
3856±3	17±2	(1010)	1010±100	35±5
3859±3	14±2			
3870±3	41±4	(7440)	7440±200	84±9
3879±3	25±3			
3904±3	54±6	(520)	520±60	138±16
3936±3	29±3			
3954±3	62±7	(5030)	5030±250	126±15
3978±3	49±5	(8170)	8170±400	99±12
3982±3	42±5			
4004±3	73±8	(3060)	3060±200	153±20

a) Note difference in Γ_n values

b) From Tellier [1971].

TABLE 6
¹⁴⁶Nd RESONANCE PARAMETERS

E (eV)	$g\Gamma_n \Gamma_\gamma / \Gamma$ (meV)	$g\Gamma_n$ (meV)	Γ_n (meV) b)	Γ_γ (meV)	ℓ^a
2585±20	85±15	(32600)	32600±500	85±15	0
2788±3	8±1	10±1 ^{b)}	65±20		1
2934±3	10±1	12±2 ^{b)}			1
2976±5	45±4	5000±1500	3580±200	45±5	0
3153±3	4±1	5±1 ^{b)}			1
3242±3	38±4	(2190)	2190±200	39±5	0
503±3	19±2	24±4 ^{b)}			1
3543±3	7±1	8±1 ^{b)}			1
3598±3	4±1	5±1 ^{b)}			1
3642±3	50±8	(25675)	2567±790	50±8	0
3833±3	11±1	15±3 ^{b)}			1
3952±5	11±2	(4910)	4910±200		0
3973±10	83±10	(12300)	12300±400		0
(4033)	-		420±60		
4069±3	11±1	15±3	320±60		0
4198±3	18±2	30±10 ^{b)}			(1)
4371±3	14±1	21±3			1
4507±3	18±2				(1)
4557±3	6±1	7±2			1
4717±3	13±1	19±3			1
5015±3	8±1	10±2			1
5064±3	70±7	(3490)	3490±150	71±7	0
5164±3	58±6	(2640)	2640±150	59±7	0
5176±3	13±1				1
5228±3	23±3	1000±500		23±10	1
5362±3	18±2				1
5389±3	12±1				1

TABLE 6 (Cont'd)

E (eV)	$g_n^{\Gamma} \Gamma_{\gamma} / \Gamma$ (meV)	g_n^{Γ} (meV)	Γ_n (meV b)	Γ_{γ} (meV)	ℓ a)
5437±3	86±9	(6370)	6370±250	87±10	0
5486±3	24±3				
5645±3	13±2				1
5870±3	7±1				1
5951±3	27±3				
6049±5	18±3				
6177±5	24±3				
6268±5	28±4				
6357±10	65±8	(10400)	10400±900	65±8	0
6598±10	43±6	(14500)	14500±790	43±6	0
6623±5	23±3				
6739±5	25±4				
6884±5	10±2				1
7010±5	40±6	(2680)	2680±150	40±6	0
7205±5	13±2				1
7251±5	30±4				
7290±5	16±2				1
7347±5	16±3				1
7372±5	29±4				
7463±5	16±3				1
7596±5	21±4				
7717±5	31±4				
7863±5	41±5				
7886±5	39±5	(3610)	3610±200	39±5	0
7931±5	31±4				
7991±5	12±3				1
8045±5	13±3				1

TABLE 6 (cont'd)

E (eV)	$g_n^{\Gamma} \Gamma_{\gamma} / \Gamma$ (meV)	g_n^{Γ} (meV)	Γ_n (meV) b)	Γ_{γ} (meV)	ℓ a)
8080±5	4±2				1
8186±5	13±3				
8466±5	27±4	(2315)	2315±225	27±5	0
8500±5	32±4				
8533±5	29±4				
8623±5	62±7				
8653±5	38±5				
9085±6	23±3				
9143±6	29±4				
9270±10	57±8	(5135)	5135±600	58±8	0
9433±6	28±4				
9543±6	33±4				
9685±6	40±5	(2100)	2100±250	40±6	0
9800±6	17±3				(1)
9813±6	47±7	(19480)	19480±1000	47±7	0

a)

ℓ -values determined from Bayes' theorem (>98% confidence level).

b) From Tellier [1971].

TABLE 7
 ^{148}Nd RESONANCE PARAMETERS

E (eV)	$g_n^{\Gamma} \Gamma_{\gamma} / \Gamma$ (meV)	g_n^{Γ} (meV)	Γ_n (meV ^d)	Γ_{γ} (meV)	ℓ^a
2710±3	14±2	22±8 ^{b)}			(1)
2772±3	11±2	12±3 ^{b)}			1
2784±3	36±4	(1410)	1410±50	37±4	0
2989±3	36±4	(2170)	2170±100	36±4	0
3045±3	2±1	2±1 ^{b)}			1
3065±3	6±1	7±2 ^{b)}			1
3121±3	24±3				
3170±3	20±2				
3355±3	12±2	17±5 ^{b)}			1
3442±3	7±1	8±1 ^{b)}			1
3484±3	30±3	(665)	665±30	31±5	0
3612±3	6±1	7±1 ^{b)}			1
3645±3	28±3				
3769±3	4±1	5±1 ^{b)}			1
3812±3	29±3	(430)	430±30	31±4	0
3837±3	9±1	12±3 ^{b)}			1
3891±10	34±4	2500±500 ^{c)}	19150±750	35±5	0
3972±3	3±1	4±1 ^{b)}			1
3948±3	4±1	4±1 ^{b)}			1
4027±3	9±1	12±1 ^{b)}			1
4073±10	66±7	(17545)	17545±400	67±7	0
4145±3	11±1	15±5 ^{b)}			1
4267±5	46±5	(7200)	7200±400	46±5	0
4307±3	11±2	16±5 ^{b)}			1
4403±3	7±1	8±1 ^{b)}			1
4420±5	47±5	2500±500	1490±75	47±5	0
4442±3	7±1	8±1 ^{b)}			1

TABLE 7 (Cont'd)

E (eV)	$g\Gamma_n \Gamma_\gamma / \Gamma$ (meV)	$g\Gamma_n$ (meV)	Γ_n (meV; d)	Γ_γ (meV)	g^a
4522±3	3±1	4±1 ^{b)}			1
4565±3	2±1	2±1 ^{b)}			1
4619±3	11±2	15±1 ^{b)}			1
4653±6	38±4	(4865)	4865±250	38±4	0
4691±3	35±4	(900)	900±50	37±5	0
4807±3	3±1				1
4838±3	23±2	(45)	45±7.5	(46)	(0)
5041±3	19±2				
5068±3	22±3				
5222±3	12±2	18±7 ^{b)}			1
5292±3	41±4	(3775)	3775±150	41±4	0
5302±3	16±2				
5401±3	23±3				
5460±3	32±4	(1590)	1590±150	32±4	0
5632±3	5±1	6±1 ^{b)}			1
5669±3	81±8	4000±1000 ^{c)}	1030±75	83±8	0
5788±3	30±4	(255)	255±90	34±6	0
5933±3	23±3				
5964±3	15±2				
6068±5	6±2	8±3 ^{b)}			1
6093±8	45±5	(5355)	5355±250	46±6	0
6133±5	5±2	6±2 ^{b)}			1
6165±5	4±2	4±2 ^{b)}			1
6213±5	3±1	4±1 ^{b)}			1
6313±5	10±2	14±4 ^{b)}			1
6343±5	23±3				
6415±5	9±2	12±3 ^{b)}			1

TABLE 7 (Cont'd)

E (eV)	$g\Gamma_n \Gamma_\gamma / \Gamma$ (meV)	$g\Gamma_n$ (meV)	Γ_n (meV) d)	Γ_γ (meV)	ℓ a)
6460±5	5±2	6±2 ^{b)}			1
6490±5	37±4	(495)	495±100	40±5	0
6545±5	2±2	2±2 ^{b)}			1
6620±5	12±2	18±5 ^{b)}			1
6640±5	39±5	(3670)	3670±150	39±5	0
6763±5	24±3				
6783±5	19±3				
6860±5	12±2	17±4 ^{b)}			1
6925±5	3±2	3±2 ^{b)}			1
6968±5	6±2	8±3 ^{b)}			1
7058±10	50±7	(14090)	14090±500	50±7	0
7100±5	21±3				
7133±5	13±2	20±6 ^{b)}			1
7195±5	26±3				
7240±5	11±3	16±5 ^{b)}			1
7303±8	80±9	6000±1000 ^{c)}	4000±200	82±9	0
7370±5	47±5	(2805)	2805±200	48±5	0
7505±5	22±3				
7545±5	22±4				
7586±5	32±4				
7668±15	67±8	(14000)	14000±500	67±8	0
7710±5	8±2	11±4 ^{b)}			1
7798±5	18±3				
7893±5	6±2	8±3 ^{b)}			1
7950±5	26±4				
7978±5	28±4				

a) ℓ -value from Bayes' theorem (>98% confidence level).

b) $g\Gamma_n$ calculated assuming $\langle \Gamma_\gamma \rangle_p = 40$ meV.

c) Note difference in $g\Gamma_n$ values.

d) From Tellier [1971].

TABLE 8
AVERAGE RESONANCE PARAMETERS

	¹⁴² Nd	¹⁴³ Nd	¹⁴⁴ Nd	¹⁴⁵ Nd	¹⁴⁶ Nd	¹⁴⁸ Nd	¹³⁸ Ba
$\langle D \rangle_s$ (eV)	680±130	35±4	450±110	19±2	270±60	170±35	7500±1500
$\langle \Gamma_{\gamma s} \rangle$ (meV)	78±10 ^{a)}	86±9	47±5	87±9	51±6	46±5	310±45
S.D. (meV)	75 ^{a)}	15	15	30	22	13	
$\langle \Gamma_{\gamma p} \rangle$ (meV)	46±5						
S.D. (meV)	~15						
$10^4 S_0$	1.40±0.35	3.1±0.5	3.9±1.0	5.2±0.9	3.7±1.0	2.7±0.8	0.9±0.4
$10^4 S_1$	1.0±0.4	1.2±0.5 ^{c)}	0.9±0.4		0.95±0.35	0.60±0.20	~0.5
$\rho(\Gamma_n^0, \Gamma_{\gamma s})$	0.90 ^{a)}	(0.41) ^{d)}	0.39	(0.44) ^{d)}	0.45	0.51	0.67
Number($\ell=0$)(obs)	24	61	17	67	21	27	
Number($\ell=0$)(calc)	35 ^{b)}	68 ^{b)}	21 ^{b)}	75 ^{b)}	22 ^{b)}	29 ^{b)}	
$\langle \sigma \rangle$ (30 keV)(mb)	77±15	175±75	84±20		123±30	113±20	5±2

a) The radiative width for the 30.6 keV resonance is six times the average; for the 13.6 keV resonance it is three times the average.

b) Calculated from fit to Porter-Thomas distribution.

c) Assuming $\langle \Gamma_{\gamma p} \rangle = 85$ meV and correcting for missed levels.

d) Obtained assuming $g = 0.5$.

TABLE 9


THE LEVEL DENSITY PARAMETER CALCULATED

FOR THE ISOTOPES OF NEODYMIUM

Isotope	<D> eV	a (MeV) ⁻¹	
		Present Data	Data of Karzhavina <i>et al.</i> [1969]
¹⁴² Nd	680	16.72±0.50	17.3±0.5
¹⁴³ Nd	35	16.58±0.18	17.7±0.4
¹⁴⁴ Nd	450	18.84±0.58	18.2±0.4
¹⁴⁵ Nd	19	18.92±0.20	19.1±0.4
¹⁴⁶ Nd	270	21.45±0.65	23.0±0.5
¹⁴⁸ Nd	170	24.48±0.71	25.4±0.5

TABLE 10

CALCULATED q_{ij} (Equation (1)) and Q_i (Equation (2)) for ^{142}Nd

Transition	$4s_{1/2} \rightarrow 3p_{3/2}$	$4s_{1/2} \rightarrow 3p_{1/2}$
E_j (calc) (MeV)	-3.54	-2.66
S_0 (calc) $\times 10^4$	← 1.67 →	
$q_{ij}^{a)}$ $\times 10^4$	22.4	13.4
$Q_i^{a)}$	 0.035	

a) for E_γ in MeV, $\Gamma_n^0, \Gamma_\gamma^V$ in eV.

TABLE 11

CALCULATED VALENCE RADIATIVE WIDTHS FOR
SELECTED RESONANCES IN THE Nd ISOTOPES
COMPARED WITH THE AVERAGE

	^{142}Nd	^{143}Nd	^{144}Nd	^{145}Nd	^{146}Nd	^{147}Nd
E (eV)	30610	2761	6788	2839	3642	4073
Γ_n (eV)	364.65	6.34	48.0	3.0	25.675	17.545
Γ_n^0 (eV)	2.08	0.12	0.58	0.06	0.43	0.27
$\Gamma_{\gamma i}^V$ (meV)	73	~4	~20	~2	~15	~10
Γ_Y (meV)	435	100	45	167	50	67
$\langle \Gamma_Y \rangle$ (meV)	78	86	47	87	51	46
$\langle \Gamma_{\gamma i}^V \rangle$ (meV)	3	~0.4	~6	~0.3	~3	~2

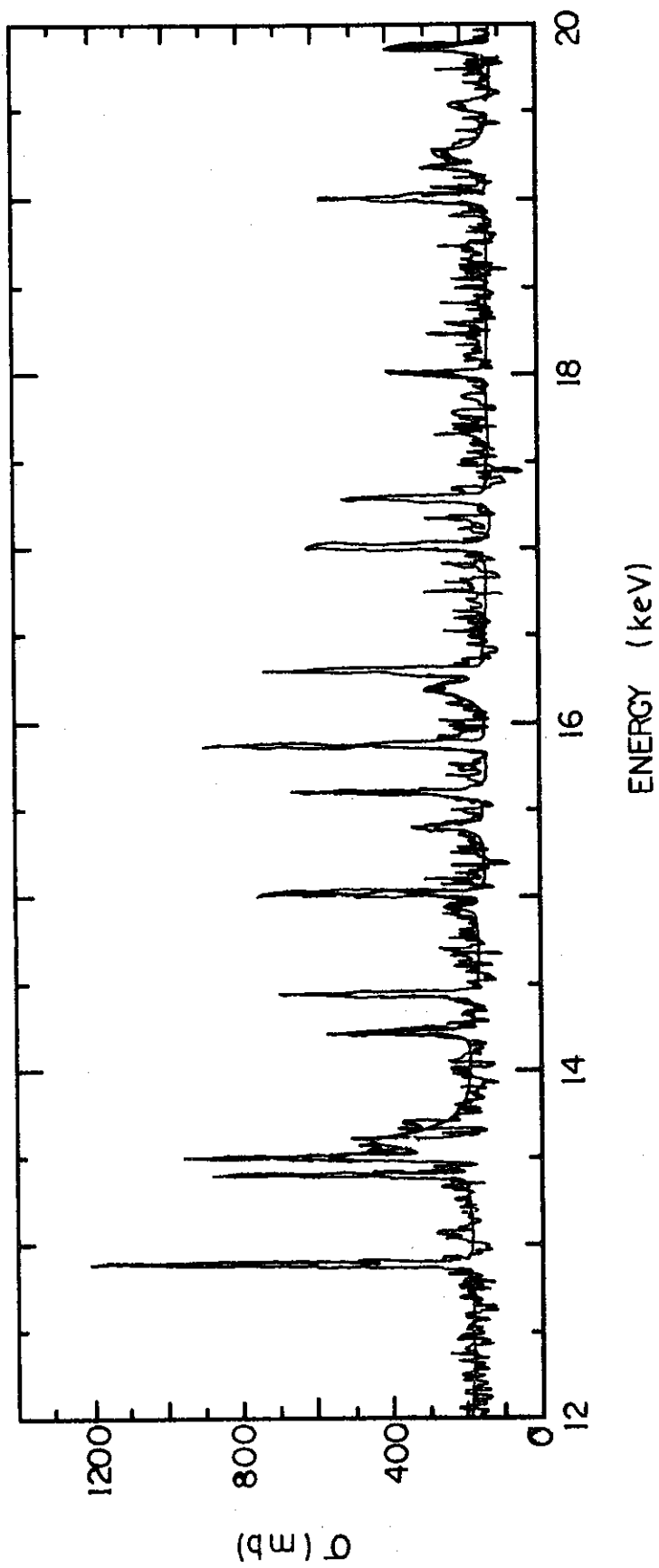


FIGURE 1. FIT TO EXPERIMENTAL DATA FOR $^{142}\text{Nd}(n,\gamma)$ BETWEEN 12 AND 20 keV.

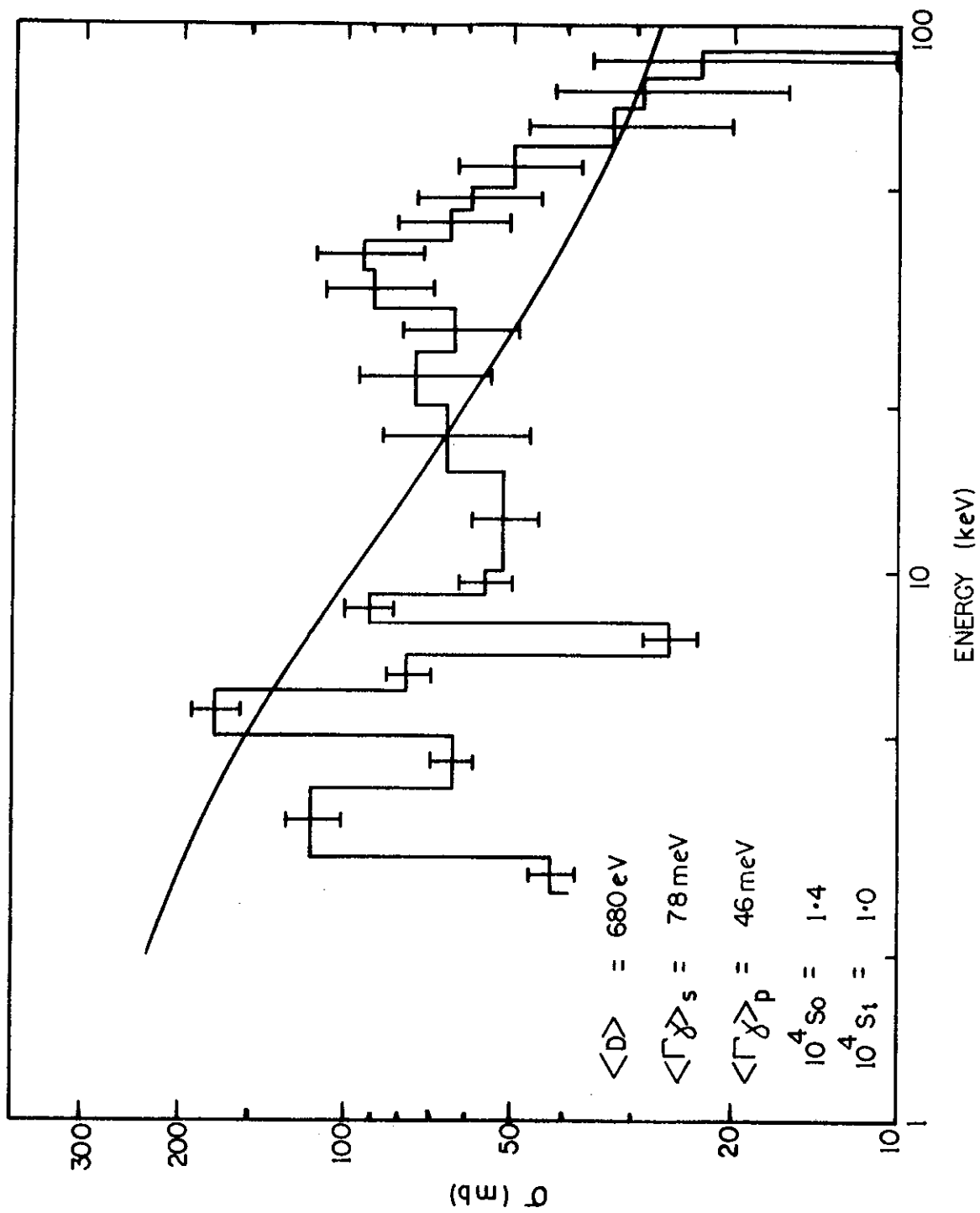


FIGURE 2 . CROSS SECTION FOR $^{142}\text{Nd} (n,\gamma)$ COMPARED WITH STATISTICAL MODEL CALCULATION

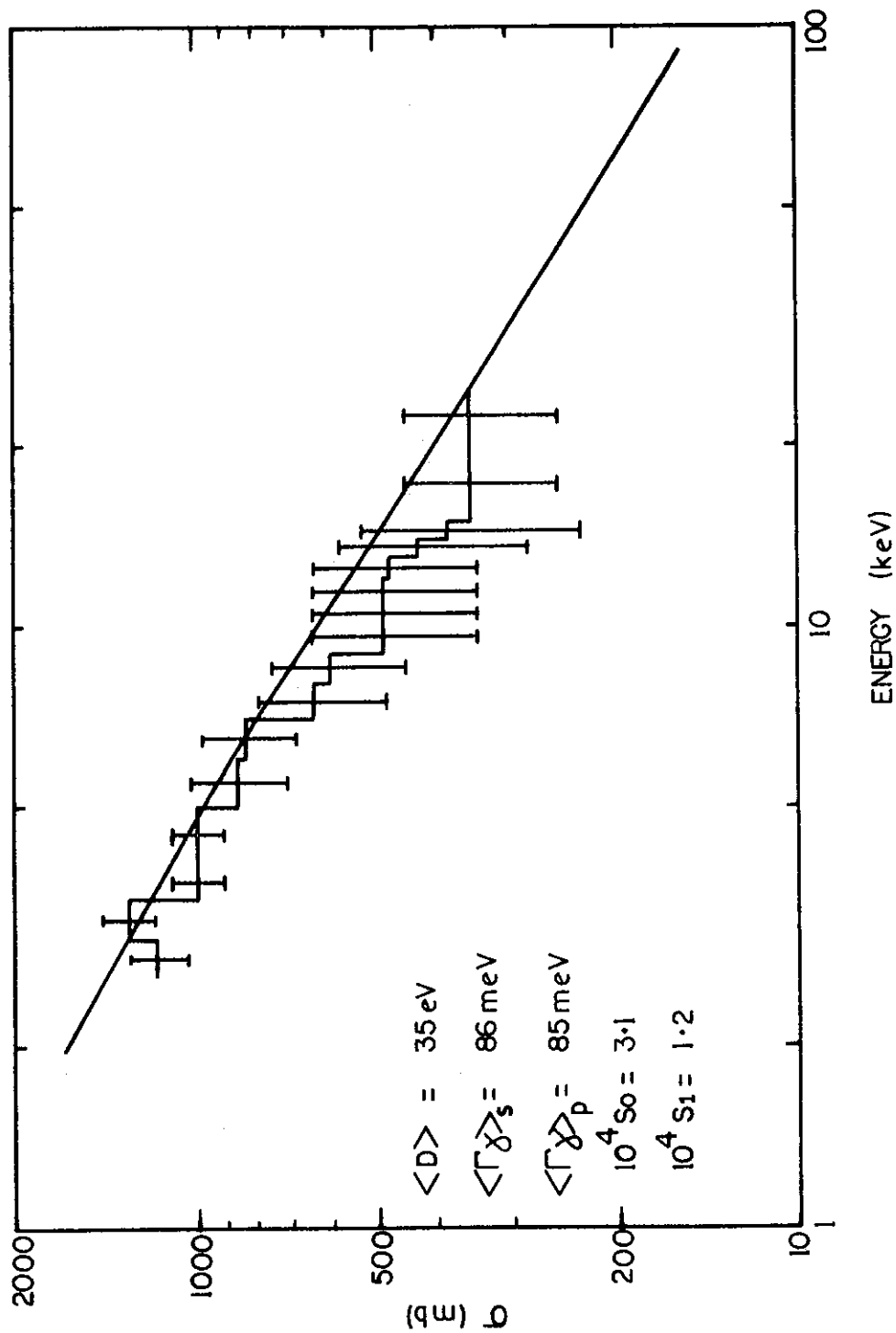


FIGURE 3. CROSS SECTION FOR ^{143}Nd (n, γ) COMPARED WITH STATISTICAL MODEL CALCULATION

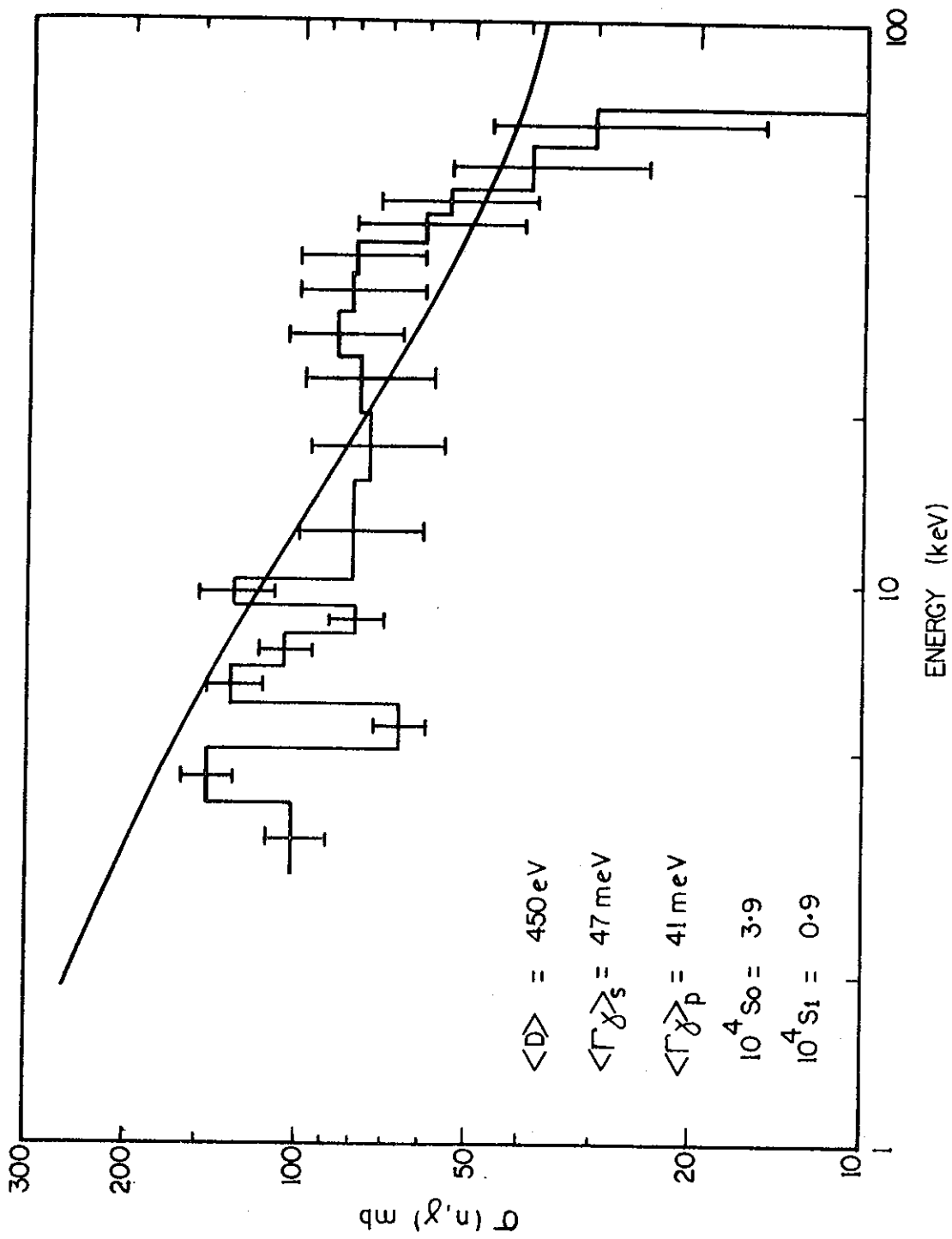


FIGURE 4 . CROSS SECTION FOR $^{144}\text{Nd} (n, \gamma)$ COMPARED WITH STATISTICAL MODEL CALCULATION

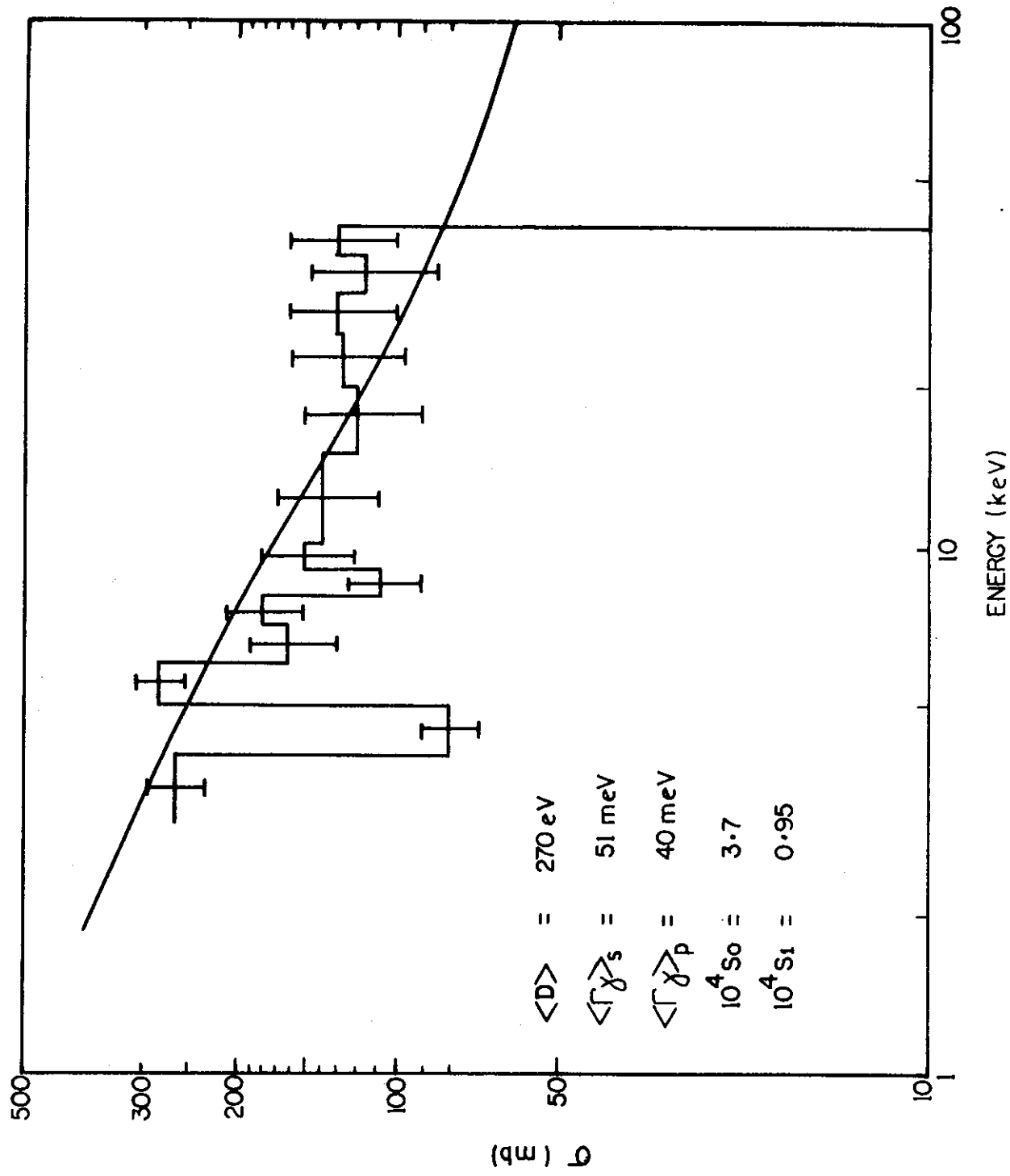


FIGURE 5. CROSS SECTION FOR $^{146}\text{Nd} (n,\gamma)$ COMPARED WITH STATISTICAL MODEL CALCULATION

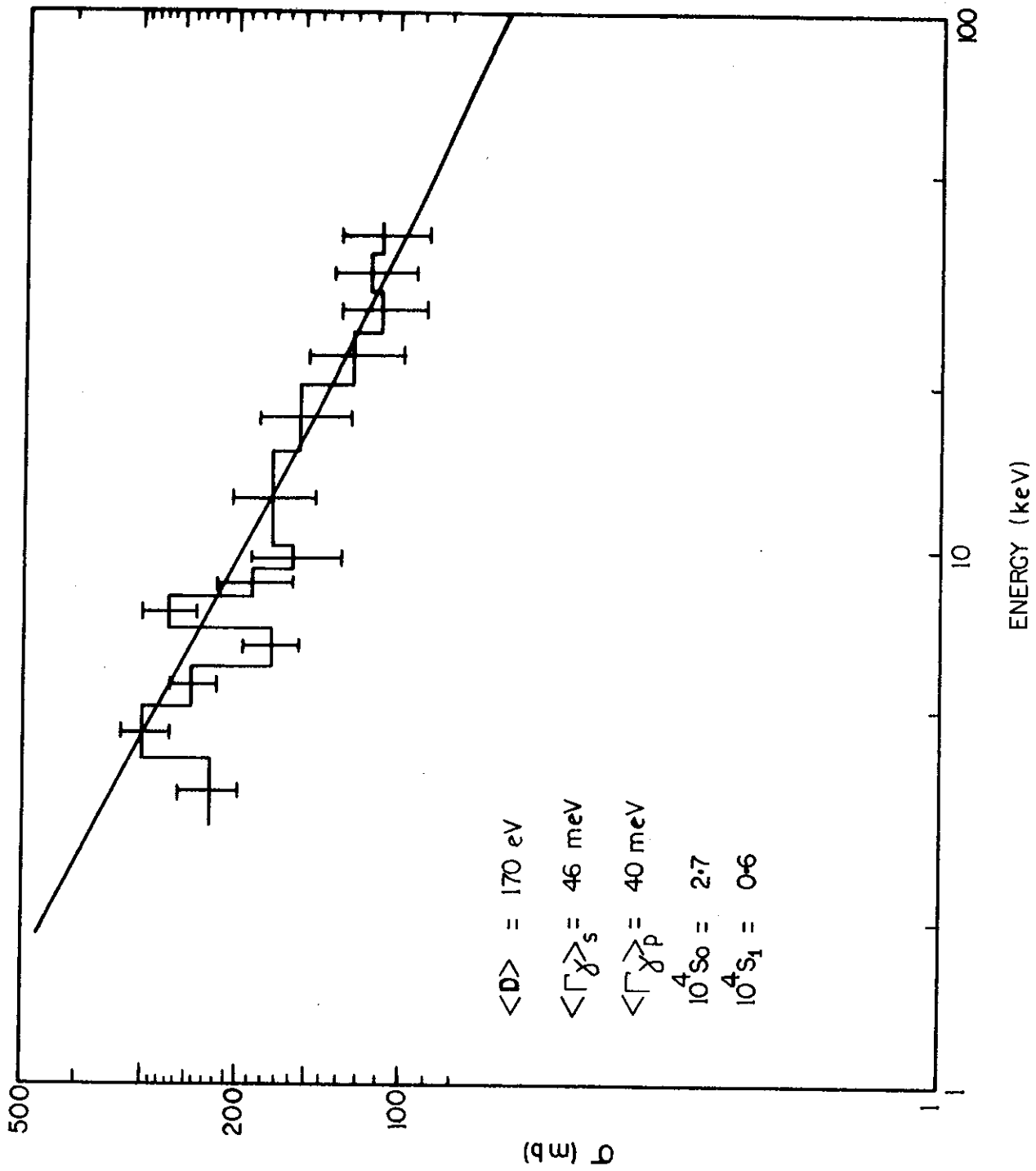


FIGURE 6. CROSS SECTION FOR $^{148}\text{Nd} (n, \gamma)$ COMPARED WITH STATISTICAL MODEL CALCULATION.

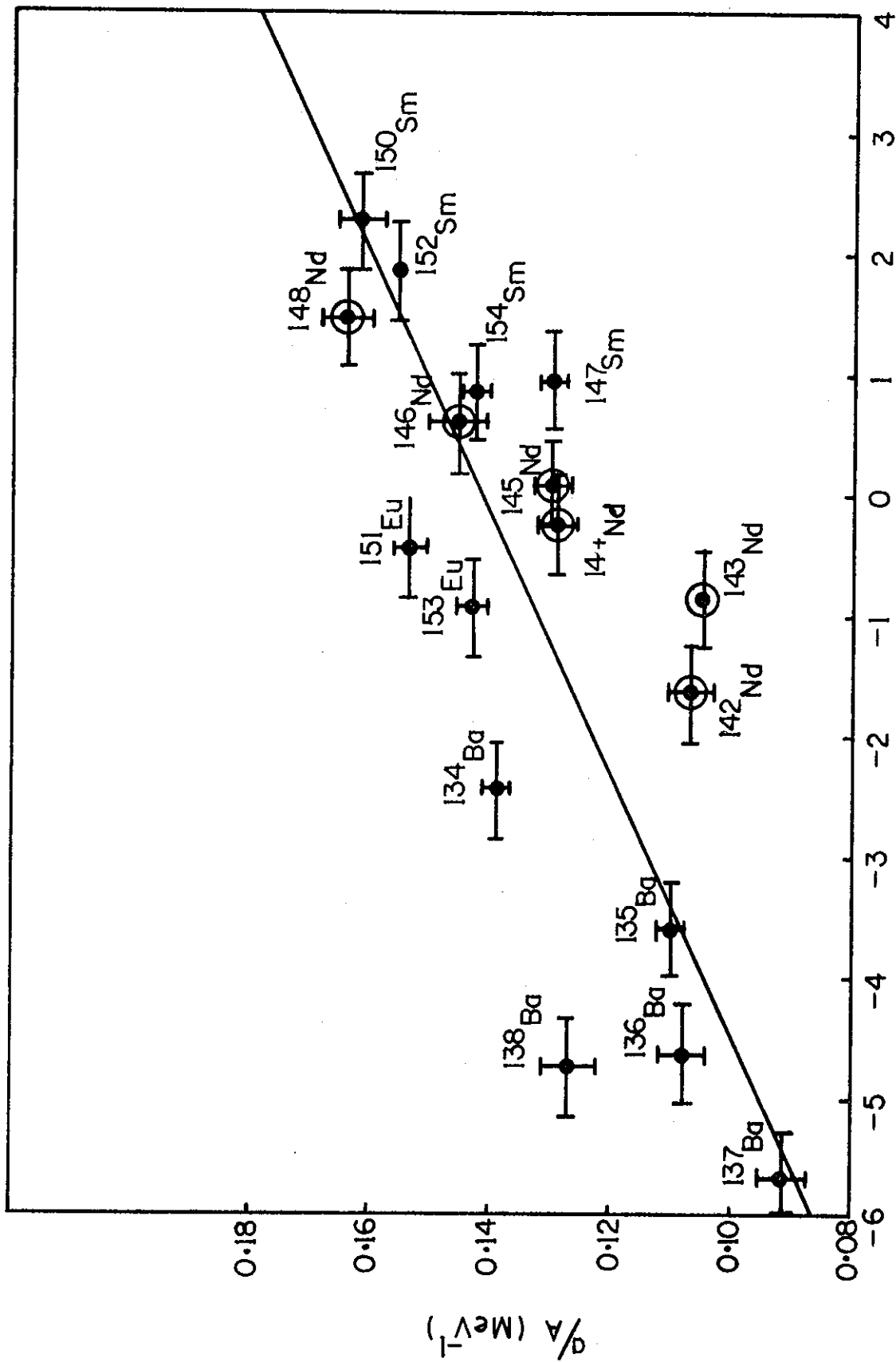


FIGURE 7. LEVEL DENSITY PARAMETER a/A VERSUS THE CAMERON SHELL CORRECTION ENERGY. ALSO SHOWN IS THE GILBERT & CAMERON GLOBAL FIT FOR UNDEFORMED NUCLEI.

